LASER & PHOTONICS REVIEWS
www.lpr-journal.org

Nonlinear Dielectric Nanoresonators and Metasurfaces: Toward Efficient Generation of Entangled Photons

*Polina R. Sharapova, Sergey S. Kruk, and Alexander S. Solntsev**

Among the most prominent effects resulting from nonlinear light–matter interaction is the generation of correlated and entangled photons through various processes, notably via spontaneous parametric down-conversion or spontaneous four-wave mixing. Such nonlinear optical processes benefit from the concentration of electromagnetic fields in small volumes. Dielectric nanoresonators and their 2D layouts—metasurfaces—provide efficient ways to control light in subwavelength volumes enabling the enhancement of nonlinear light–matter interaction and the generation of entangled photons. Nanoresonators and metasurfaces offer a radical miniaturization of quantum light sources allowing better scalability, which opens a pathway toward arrangements of photon sources in complex subwavelength configurations for advanced photon state control. In this work, the recent progress in this emergent area of research is reviewed.

1. Introduction

Quantum photonics has the potential of revolutionizing technology by bringing quantum effects toward applications. An important basis for many applications in communication, sensing, and computing are tailored photonic quantum states.[1–5] Among the most prominent sources of such states are nonlinear optical systems generating photon pairs, states containing exactly two photons which are called signal and idler, through spontaneous nonlinear processes. Depending on the used nonlinear material, two different processes can be employed: spontaneous parametric down-conversion (SPDC) and spontaneous four-wave mixing (SFWM). SPDC is possible in materials with broken inversion symmetry featuring a second-order nonlinearity.[6] In this parametric three-wave mixing process, pump photons spontaneously decay into pairs of signal and idler photons. In materials with inversion symmetry, photon pairs can be generated SFWM where now two pump photons are converted into photon pairs.[7] Both SPDC and SFWM are governed by similar rules. First, energy conservation determines the possible frequencies of the signal and idler photons, as their sum has to be the same as for the pump photon(s). On the other hand, field matching, which for propagating waves corresponds to phase matching, determines the efficiency of the generation for certain sets of properties of the photon pairs, for example, frequency, polarization, and propagation direction, which are compatible with energy conservation.

This enables far reaching and versatile possibilities to control the properties of photon pairs by a suitably designed nonlinear optical system that controls the fields of the pump, signal, and idler waves. Such control allows the production of pure and indistinguishable heralded single photons[8] and correlated pairs of photons,[9,10] which have numerous applications in quantum optics. Among the nonlinear optical structures used for controlling the properties of generated photon pairs are suitably cut bulk crystals, waveguides, and optical fibers, as well as resonators.[6,7,11–15] In the past, control of the polarization, spectrum, spatial composition, and degree of entanglement were demonstrated based on the principles of tailoring propagating fields within nonlinear systems that were much longer than the wavelength of light.[9,16]

In the last years, a different paradigm for controlling both linear and nonlinear light–matter interaction has seen a rapid development: Resonant dielectric nanostructures and metasurfaces have demonstrated remarkable capabilities of controlling virtually every parameter of the electromagnetic field via carefully engineered geometrical resonances at the subwavelength scale. Dielectric nanostructures can feature Mie-type modes and composite resonances with local field distributions and resonance frequencies delicately dependent on the nanoresonator geometry.[17–24] Arranged in 2D arrays, often termed metasurfaces, such structures have been used to create ultra-thin functional optical components, including lenses,[25] polarization

P. R. Sharapova, S. S. Kruk
Department of Physics
Paderborn University
33098 Paderborn, Germany

S. S. Kruk
Research School of Physics
Australian National University
Canberra, ACT 2601, Australia

A. S. Solntsev
School of Mathematical and Physical Sciences
University of Technology Sydney
Sydney, NSW 2007, Australia
E-mail: alexander.solntsev@uts.edu.au

The ORCID identification number(s) for the author(s) of this article can be found under https://doi.org/10.1002/lpor.202200408

DOI: 10.1002/lpor.202200408

converters,[26] and holograms[27] among others. Metasurfaces have been employed to control quantum light, both for detection and to imprint a specific quantum state in photon pairs generated in a bulk nonlinear crystal.[5,28]

This control of light propagation using dielectric nanoresonators and metasurfaces has been recently also extended to nonlinear light generation and control by using parametric frequency conversion.[29–34] Here, resonant field enhancement enables significant improvement of conversion efficiencies while control of the field profile allows one to tailor the properties of the generated light.

Resonant dieielctric nanophotonics holds great promise for the generation of entangled photon pairs, as it offers a high level of control over the properties of generated photons via the nanostructure geometry. This may lift some restrictions present in established optically large photon-pair sources, including those associated with the need for phase matching or limited available material properties in waveguides and bulk crystals.

Here, we give an overview about the first steps into this promising direction. First, we will very briefly review the state of the art in classical nonlinear optics of nanoresonators and metasurfaces. Then, we will discuss how these advancements in classical nonlinear nanophotonics can be related to quantum light sources and cover most recent progress on photon-pair generation in nanoscale subwavelength systems, including individual AlGaAs nanoresonators as well as lithium niobate metasurfaces before concluding with an outlook.

2. Classical Nonlinear Optics in Dielectric Nanostructures

Generation of entangled photons via spontaneous parametric down conversion (SPDC) can be considered as a process reversed to classical nonlinear generation of parametric waves. The direct correspondence between the SPDC process and the sum frequency generation (SFG), as well as the second-harmonic generation (SHG) has been rigorously proven in [35]. We envision future studies of rigorous correspondences between broader classes of classical nonlinear wave mixing processes and generation of entangled quantum states. It is therefore illustrative to overview the recent developments of classical nonlinear optics in dielectric nanostructures as an outlook for possible future research directions for the generation of entangled photon states.

Conventional nonlinear optical systems typically require bulk volumes of a material, often combined with a confining cavity. This increases the photon lifetime, thus strengthening light–matter interactions. In a striking contrast to these conventions, the recent developments of resonant dielectric nanostructures facilitating strong light concentrations opened the path toward efficient nonlinear processes on a scale smaller than the wavelength of light.

High refractive index nanoparticles with carefully engineered geometries can support multiple different types of optical modes, including optically induced magnetic dipole (MD) resonances,[36] higher-order multipoles,[37] anapole modes,[38] and modes associated with bound states in the continuum[39] among others. High field enhancements near the magnetic dipole modes and composite resonances increase the efficiency of nonlinear processes by orders of magnitude. In striking contrast to nonlinear light–matter interactions in bulky media which are governed by phase-matching requirements, the phase matching plays no role in subwavelength resonators hosting localized modes. The nonlinear light–matter interaction depends on the field confinement (the Q-factors of the resonances) and on the overlap of modes at the frequencies involved in the nonlinear process.

Nonlinear optics at the nanoscale has seen a tremendous progress in recent years with a steady increase in nonlinear conversion efficiencies. Originally, it was associated with short laser pulses with typical durations on the order of tens and hundreds of femtoseconds. Such short pulses may reach high levels of peak power, thus enhancing nonlinear light–matter interaction while minimizing parasitic effects such as heating and free-carrier dispersion. However, recent developments in high-Q metasurfaces have enabled nonlinear light–matter interaction between nanostructures and continuous-wave (CW) lasers with much lower peak powers compared to their pulsed counterparts.[40] Generation of the second harmonic from metasurfaces in CW regime is one manifestation of the progress being made in subwavelength nonlinear optics. Below, we overview some recent research on classical nonlinear nanoresonators and metasurfaces.

In the recent past, several different strategies have been explored for the enhancement of nonlinear light–matter interaction in subwavelength resonators via engineering of their optical modes.[24] **Figure 1**a (left) shows a concept image of an individual subwavelength resonator for the second harmonic generation.[39] At its resonant condition, the resonator increases the efficiency of second harmonic generation by orders of magnitude as seen in Figure 1a (right). The conversion efficiency in this resonator, defined as the peak power of the second harmonic divided by the peak power squared of the optical pump, or fundamental field $P^p_{SH}/(P^p_{FF})^2$, was estimated to reach 10^{-6} W^{-1}. The resonator was fabricated from AlGaAs material and was optically pumped in the spectral region of optical fiber communications at around 1600 nm wavelength.

Nanoscale photonics has seen exciting new developments in the regimes of ultra-high optical fields reaching the regimes of nonperturbative nonlinearities. Nonlinear light–matter interaction at the nanoscale studied originally were sufficiently weak to be considered only as small perturbations to the linear regime (and hence were described within the framework of perturbative nonlinear optics). However recently, intense light–matter interaction going beyond the perturbative approach have been studied in nanoresonators. A striking effect arising from nonperturbative interactions is the high harmonics generation (HHG).[45] For decades, the HHG was associated with media in gas and plasma states, and only recently, generation of high-order optical harmonics entered the realm of nanostructured solids. Processes of high harmonic generation might be of a particular interest to explore, since such systems with high nonlinearity might potentially be useful for simultaneous generation of multiple correlated photons. This in particular might open a door to efficient squeezed light generation on the nanoscale. Figure 1b shows an example of generation of up to seventh optical harmonic from an individual subwavelength AlGaAs resonator.[41] In this demonstration, the resonator was optically pumped with a mid-infrared light source, and optical harmonics were observed in the near-infrared and the visible spectral ranges.

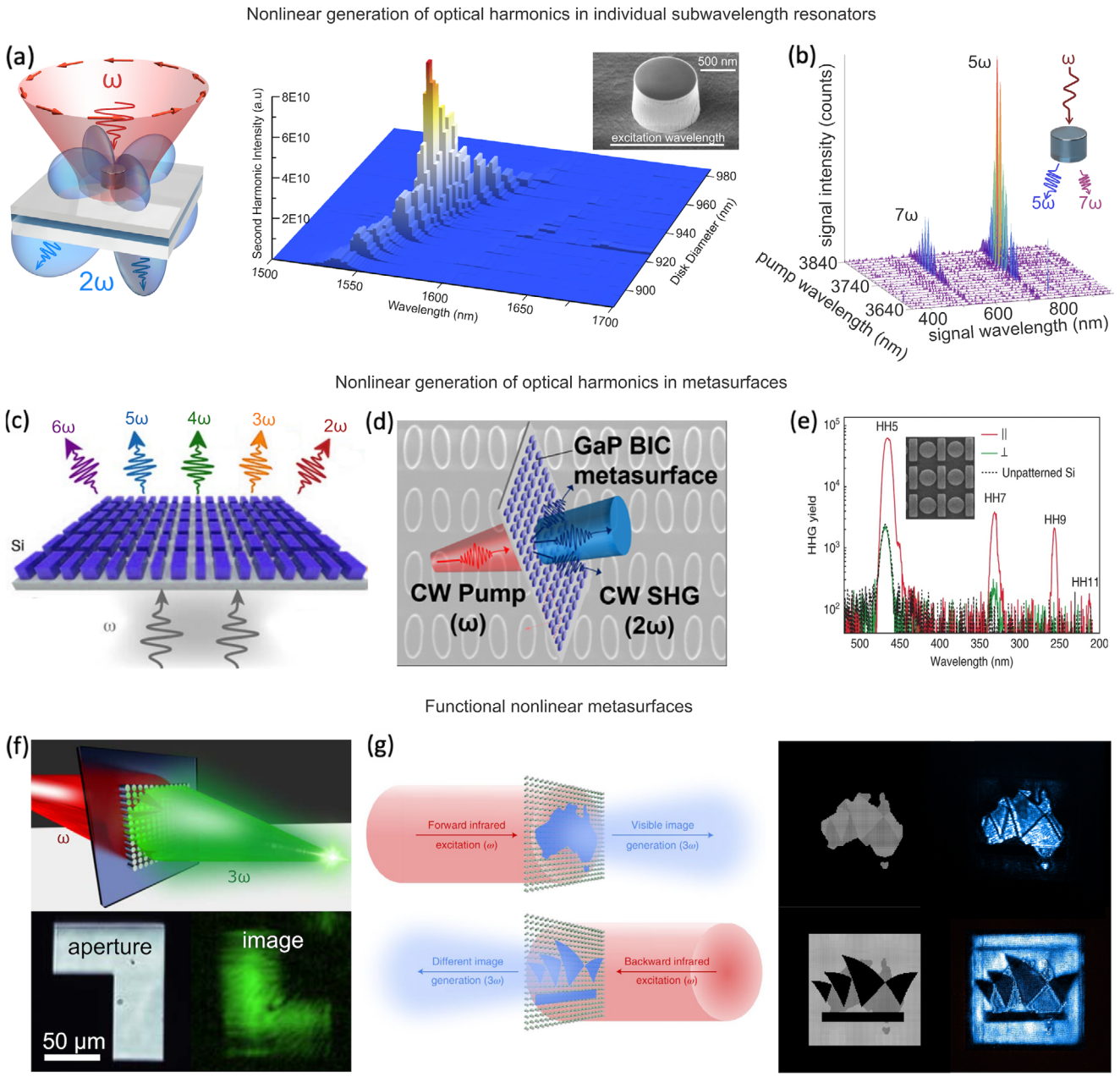

Figure 1. Subwavelength dielectric photonics for enhanced nonlinear light-matter interaction. a) Generation of second optical harmonic in an individual nanoresonator. The harmonic generation is enhanced by orders of magnitude at a resonance associated with bound states in the continuum. Adapted with permission.[39] Copyright 2020, American Association for the Advancement of Science. b) Generation of high optical harmonics in an individual subwavelength resonator. Adapted with permission.[41] Copyright 2022, Optica Publishing Group. c) A concept image of harmonics generation in a dielectric metasurface. d) Generation of second optical harmonic from a metasurface pumped with a continuous-wave (CW) light source. Adapted with permission.[40] Copyright 2020, American Chemical Society. e) Generation of high optical harmonics from a metasurface. Adapted with permission.[42] Copyright 2018, Nature Publishing Group. f) A nonlinear metasurface acting as an upconversion lens imaging objects at the third harmonic frequency. Adapted with permission.[43] Copyright 2020, American Chemical Society. g) A nonlinear metasurface producing different images for the opposite direction of illumination. Adapted with permission.[44] Copyright 2022, Nature Publishing Group.

2D layouts of nanoresonators assembled on a subwavelength scale and often referred to as metasurfaces offer new opportunities to enhance and to control nonlinear light–matter interaction. Collective optical modes in metasurfaces allow us to achieve spectrally narrow optical resonances with high quality factors (Q-factors). Such modes can be engineered by employing frameworks of Fano-resonances,[46] electromagnetically induced transparency,[47] and symmetry protected bound states in the continuum (BICs)[48] among others. Remarkably, such high-Q collective modes enabled the transition of nonlinear nanophotonics from pulsed to continuous-wave regime. In a recent paper, gallium phosphide metasurfaces with Q-factors up to $Q = 2 \times 10^3$

have been used for second harmonic generation. The high Q-factor enabled the observation of nonlinear frequency conversion in both femtosecond and CW regimes[40] (Figure 1d). It was shown that the increase in the Q-factor in the CW regime consistently improved the nonlinear response of the structure. This is of potential importance for the reverse process of SPDC, in which the generated photon rate scales linearly with the pump, and hence, CW regime is often desirable. The CW regime would bring multiple benefits to the SPDC at the nanoscale. Despite being the second-order nonlinear process, SPDC scales linearly with the excitation power, which relieves the requirements for the high peak power values. This mitigates problems with the pulsed excitation that might induce parasitic nonlinear effects and reach peak intensities above the laser damage threshold. CW excitation further allows for spectrally narrow excitation which plays an important role in coupling to high Q-factor (and thus spectrally narrow resonances).

Generation of high-order optical harmonics in all-dielectric metasurfaces has been demonstrated in the recent years. One of the pioneering works demonstrated HHG in dielectric metasurfaces hosting resonances associated with electromagnetically induced transparency[42] (Figure 1e). HHG in metasurfaces hosting bound states in the continuum was demonstrated recently in ref. [49]. In this work, a set of metasurface hosting detuned quasi-BIC modes was developed, which allowed tracing transitions between perturbative and non-perturbative nonlinear regimes experimentally. A striking advantage of solid-state HHG compared to its conventional counterparts of HHG in gases is the ability to employ non-centrosymmetric media for the generation of even-order harmonics. Recently, a metasurface made of a non-centrosymmetric material GaP enabled the generation of both even and odd high harmonics.[50] Even-order optical harmonics up to sixth order and odd harmonics up to ninth order have been observed.

Metasurfaces assembled from dissimilar nanoresonators provide opportunities for spatially inhomogeneous control of light, including the control of nonlinearly generated parametric waves. Nonlinear optics changes the basic principles of interaction between light and matter, including the superposition principle, geometric optics approximation, and optical reciprocity enabling novel properties and functionalities. Nonlinear light–matter interaction in metasurfaces have been utilized recently to expand the range of applications of metasurfaces beyond the limitations of their linear counterparts.

Recently, all-dielectric nonlinear metasurfaces were used as upconversion lenses for imaging of objects.[43] The objects were illuminated with intense near-infrared radiation, and the lenses were building their images in the visible spectral range (Figure 1f). Interestingly, the nonlinear image formation studied phenomenologically was not grasped by conventional lens equations routinely used in linear optics, and modified nonlinear lens equations were suggested. Moreover, since the superposition principle of waves does not hold in the regime of nonlinear optics, such lenses were also demonstrating image formations accompanied by the autocorrelation function of the order of optical harmonics, thus carrying information about the spatial coherence of light.

Nonlinear light–matter interaction lifts several restrictions of linear optics on asymmetries in both generation and propagation of light with respect to changing the positions of transmitters and receivers. Recent research demonstrates asymmetric image formation in dielectric metasurfaces (Figure 1g).[44] When researchers were looking through the metasurface at an infrared source, they observed a certain encoded image in the visible spectral range (like looking through a photographic film slide), as sketched in the figure. However, once the metasurface was flipped, a completely different encoded image could be observed in transmission. This was achieved by controlling optical responses of individual nanoresonators constituting the metasurface. Each resonator was performing its own operation by generating either high or low intensity of light depending on the direction of illumination. This demonstration marks an important milestone in expanding the range of metasurface applications which may go beyond classical optics toward controllable asymmetric quantum light generation.

The advancements in classical nonlinear optics at the nanoscale, including the metasurfaces with nontrivial functionalities such as upconversion imaging and asymmetric control of light, embolden the vision of the development of nonlinear nanoresonators and metasurfaces for the generation of entangled photon states with embedded functionalities for controlling the properties of the photons.

3. Spontaneous Parametric Down-Conversion and Generation of Non-Classical Light

Efficient classical nonlinear frequency conversion and generation of optical harmonics imply reverse quantum regimes with bright photon-pair generation. In particular, there is a direct correspondence between sum-frequency generation (or SHG in the degenerate regime), and a reverse quantum process SPDC.[35] Thus, Mie resonators optimized for efficient SHG can also be utilized for the reverse process of SPDC, enabling the generation of entangled photon pairs on the nanoscale.[51,52] This pathway is particularly attractive as it brings nanoscale quantum light sources to room temperature, without the need for expensive and cumbersome cryogenic cooling that would be necessary when working with, for example, quantum dots.

SPDC in subwavelength Mie resonators has first been demonstrated in AlGaAs nanocylinders.[30] **Figure 2**a shows a schematic representation of an AlGaAs nanocylinder on lower-index aluminium oxide substrate, facilitating SPDC via a Mie resonant interaction between the pump and the generated signal and idler photons. Dimensions of the cylinder are chosen such that signal and idler fields are enhanced by broadband electric dipole (ED) and MD resonances, while the pump is amplified by a spectrally narrow, high quality factor ED resonance (Figure 2b). The scanning electron microscope (SEM) image of the sample can be seen in Figure 2c. The resulting coincidences between the signal and idler photons are measured by two single-photon detectors and a correlation scheme. Figure 2d shows a peak in coincidences at a time difference corresponding to the delay between the detectors, indicating simultaneous generation of two photons in a pair in the nanoscale regime via SPDC.

To increase the SPDC efficiency, possible approaches include moving to metasurface arrangements increasing the nonlinear interaction volume, and utilizing stronger resonances, such as

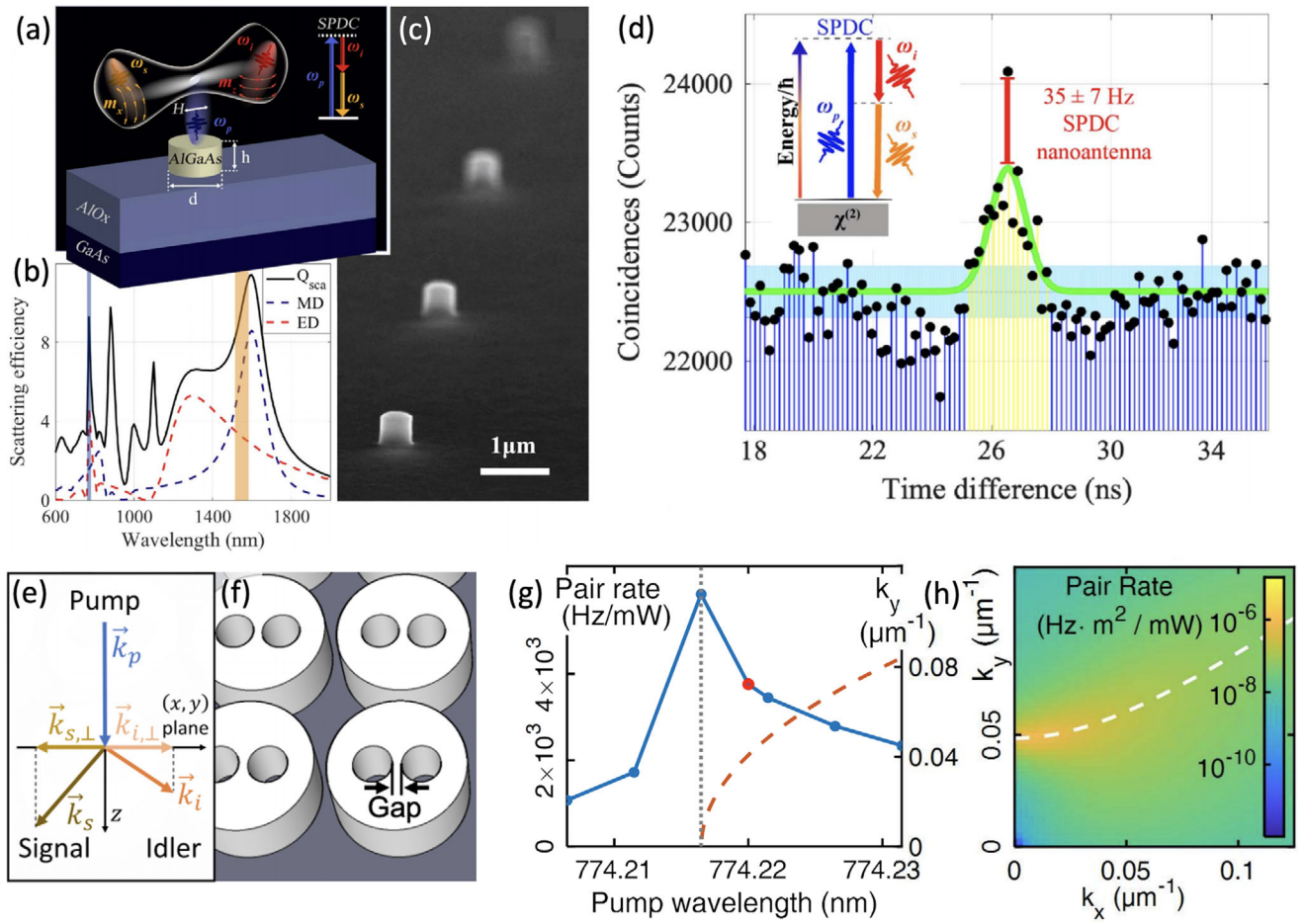

Figure 2. a) Schematic representation of the nonlinear dielectric nanoscale source of photon pairs, based on AlGaAs nanocylinder with diameter $d = 430$ nm and height $h = 400$ nm. The inset depicts the energy diagram of the SPDC process.[30] b) Simulated scattering efficiency Q_{sca} and multipolar decomposition in terms of the two leading electric and magnetic dipoles. The vertical blue and orange bars show the spectral ranges of the pump and SPDC, respectively.[30] c) Scanning electron microscope image of AlGaAs monolithic nanocylinders.[30] d) Coincidence counts on two single-photon detectors. A significant statistical increase, marked by the red bar, is apparent at a time difference of 26.5 ns, corresponding to the temporal delay between both detectors. Black dots are the measured coincidences; the green line is its Gaussian fit. The light blue shading represents the statistical error of the background. a-d) Adapted with permission.[30] Copyright 2019, Optica Publishing Group. e) Diagram of transverse phase matching.[32] f) AlGaAs metasurface design supporting BIC resonances.[32] g) Solid: SPDC generation rate versus the pump wavelength λ_p. The red dot marks the wavelength used in (h). Dashed: k_y at transverse phase matching when $k_x = 0$.[32] h) Generation rate in k-space at phase matching for $\lambda_p = 774.22$ nm. White dashed line: phase matching condition.[32] e-h) Adapted with permission.[32] Copyright 2022, IOPscience.

photonic BIC. A combination of these approaches has been theoretically investigated for SPDC in AlGaAs BIC metasurfaces.[32] Figure 2e shows wave-vectors for pump, signal, and idler angles satisfying transverse phase-matching for AlGaAs cylinders with pairs of holes shown in Figure 2f. The holes of a certain size with a particular gap between them support a strong BIC resonance in the designed metasurface. Figure 2g reveals the estimated photon-pair generation rate featuring a significant BIC-enabled SPDC efficiency enhancement. As shown in Figure 2h, in this configuration, the highest SPDC efficiency can be achieved for full phase-matching with non-zero k_x components, which would result in the generation of photon pairs at an angle to the pump beam and the plane of the metasurface. A new design intended to enhance SPDC radiation consists of a periodic arrangement of filleted nanowires, or nanofins, as presented in **Figure 3**b, and has an idea to exploit the left/right symmetry of the metasurface so as to simultaneously support two degenerate BICs, with field profiles shown in Figure 3c, for the generated photons emitted at opposite angles.

Plasmonic enhancement might also play an important role in the development of nonlinear nanoresonators and metasurfaces for the generation of entangled photons. Although dielectric nanostructures can provide higher resonant quality factors and can better withstand strong pump lasers, plasmonics allows much tighter field confinement. Recent theoretical demonstrations include a generation of $N00N$ states and a control of photon-pair correlations in individual nanoparticles[57] and two order of magnitude enhancement of the biphoton generation efficiency in plasmonic metasurfaces.[58]

Another promising material for bright SPDC generation is lithium niobate (LN), which is characterized by many fascinating properties, such as strong second-order nonlinear susceptibility

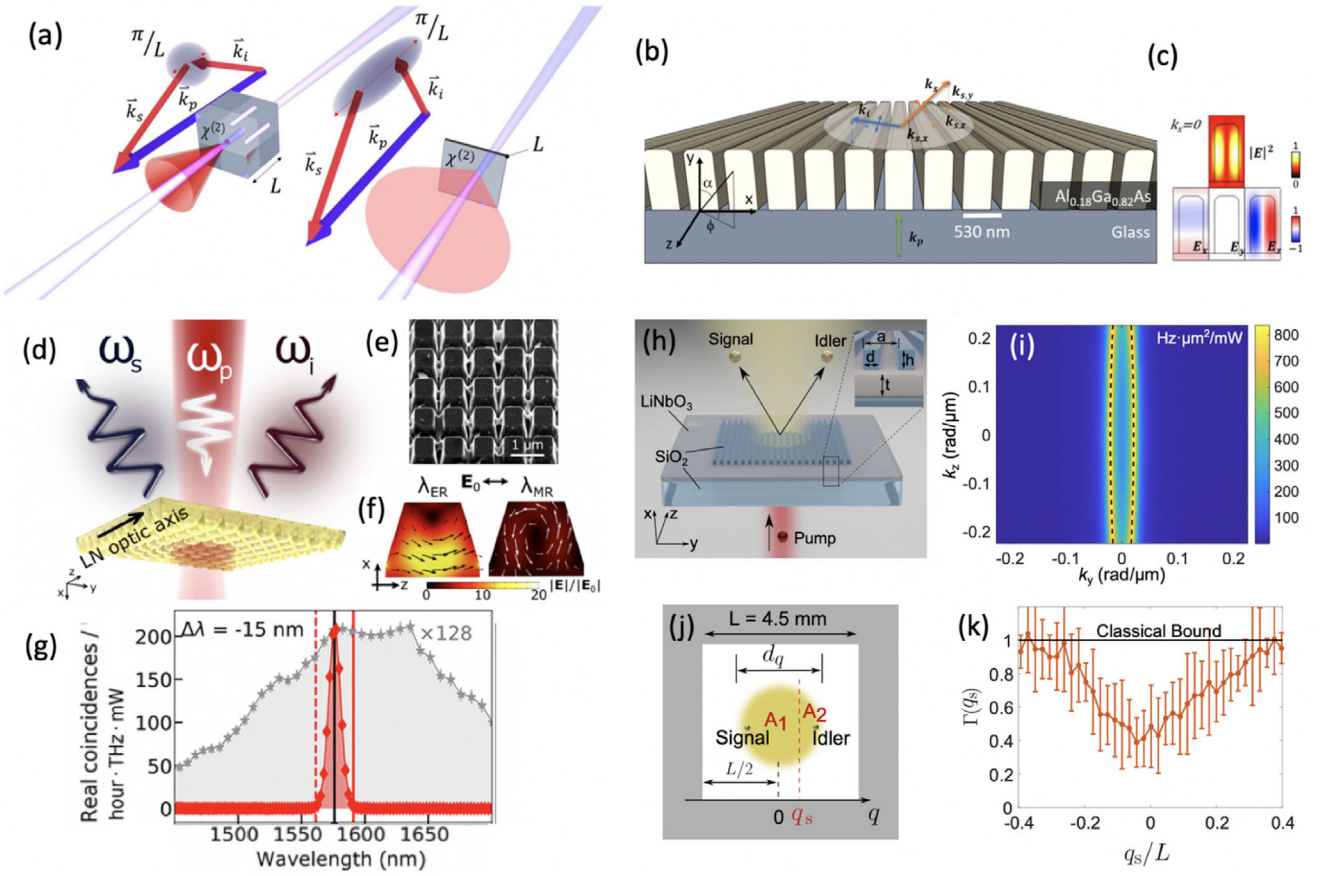

Figure 3. a) SPDC in a thick (left) and ultrathin (right) nonlinear layer of lithim niobate (LN). Reproduced with permission.[53] Copyright 2020, Springer Nature. b) Design of the metasurface made of (110)-cut $Al_{0.18}Ga_{0.82}As$ in the form of meta-grating composed of nanofins, positioned on a dielectric substrate.[54] c) Normalized field enhancement and field components patterns in correspondence of quasi-BIC resonance, sustained by the nanofins metasurface at $k_z = 0$. b,c) Reproduced with permission.[54] Copyright 2019, American Physical Society. d) Schematic representation of SPDC generation using a lithium niobate meatasurface.[55] e) Scanning electron microscopy image of a fabricated metasurface with an array of nanoresonators.[55] f) Distribution of the electric field inside a nanoresonator at the electric (λ_{ER}, left), and magnetic (λ_{MR}, right) resonances. Arrows show the electric field direction.[55] g) Measured SPDC spectrum from a metasurface with electric resonance close to the SPDC wavelengths. Gray stars show the SPDC spectrum from the unpatterned LN film. $\Delta\lambda$ indicates a difference between the resonance and SPDC wavelengths. d-g) Reproduced with permission.[55] Copyright 2021, American Chemical Society. h) Sketch of generation of spatially entangled signal and idler photons from a $LiNbO_3$ thin film covered by a SiO_2 grating and pumped by a continuous laser. Inset shows the dimensions of the metasurface (not to scale).[56] i) Predicted photon emission rate at $\omega_p/2 = 191.19$ THz as a function of transverse wavenumbers. The black dashed line indicates the momentum matching conditions for the degenerate SPDC.[56] j) A square aperture with a size of L × L is introduced after the metasurface to characterize the spatial correlations of photon pairs. The position where the centers of the beam and the aperture are aligned is defined as zero. Correlations between the spatial regions A1 and A2 separated at the position q_s are investigated and presented in (k).[56] k) Violation of Cauchy–Schwartz inequality for values below the classical bound. h-k) Reproduced with permission.[56] Copyright 2022, American Association for the Advancement of Science.

and a large transparency window. In LN, a transition to nanoscale SPDC can be performed by exploiting LN microcubes,[59] subwavelength nonlinear LN films,[53] or subwavelength thin-film lithium niobate-on-insulator (LNOI) waveguides.[60–63] In contrast to bulk crystals, thin LN slices result in SPDC, which is free of phase matching (momentum conservation) (see Figure 3a). Such quantum light sources are characterized by frequency spectrum an order of magnitude broader than that of phase-matched SPDC that leads to an increase in the number of light modes and the generation of huge frequency and angular entanglement. Thin-film LNOI waveguides, which are a subwavelength LN layer on the insulator substrate, may form the backbone of future integrated photonic circuits.[63] Unlike bulk LN waveguides, the shape of LNOI thin-film waveguides greatly affects their properties. For example, a special design of the LNOI waveguides makes it possible to generate concurrent counterpropagating SPDC processes with a single reciprocal wave vector.[62]

However, the nanoscale size of such systems challenges the efficiency of SPDC. To boost the efficiency, improved designs of thin-film LNOI waveguides have been suggested.[64,65] An alternative pathway toward higher efficiencies is to employ the concept of resonant metasurfaces,[55,56] Thus, a special engineering of nanostructured LNOI results in dispersion profiles that are different from bulk LNs; such a modification of dispersion leads to an increase of brightness of the PDC source to values comparable with bulk LN.[64] At the same time, a careful de-

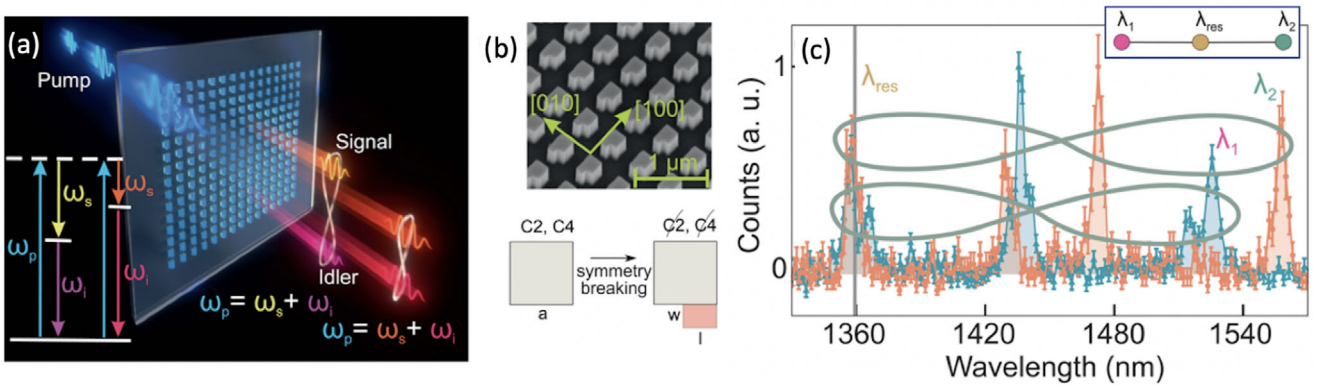

Figure 4. a) Diagram of multiplexed entangled photon generation in a multiresonance semiconductor metasurface based on GaAs.[66] b) Scanning electron microscopy image of a metasurface (top) and its broken-symmetry resonators (bottom).[66] c) Spectrum of a non-degenerate SPDC process obtained using two pump beams of different wavelengths. The signal photons of both processes (λ_{res}) are emitted at the quasi-BIC resonance. The idler photons (λ_1 and λ_2) are emitted at the correlated wavelengths determined by the energy conservation law. The spectrum illustrates how a linear three-qubit graph state of photons $|\lambda_{res}\rangle$, $|\lambda_1\rangle$, $|\lambda_2\rangle$ (shown in the insert) can be generated using quantum optical metasurface. Reproduced with permission.[66] Copyright 2022, American Association for the Advancement of Science.

sign of LNOI nanostructures can lead to the generation of signal and idler PDC photons with orthogonal polarizations but the same effective refractive indices, resulting in the production of polarization-entangled Bell-states,[65] while the maintenance of various pump modes by the waveguide can lead to multiple concurrent SPDC processes.

For the first time, the generation of SPDC photon pairs in LN-based quantum optical metasurfaces with electric and magnetic Mie-like resonances at various wavelengths has been demonstrated in ref. [55]. A general idea of SPDC generation in a metasurface in reflected geometry is shown in Figure 3d, where SPDC photons are generated in the direction opposite to the pump direction. SEM image of the fabricated LN-based metasurfaces is presented in Figure 3e. Such metasurfaces consist of an array of nanoresonators in the shape of truncated pyramid. The distribution of the electric field inside nanoresonators depends on the type of resonance and is depicted in Figure 3f, where arrows show the electric field direction. The resonances characterizing the metasurface can be shifted by varying the size/period of the pyramidal nanoresonators. The SPDC spectrum for the metasurface with a resonance close to the PDC wavelength is presented in Figure 3g and shows a giant enhancement of SPDC rate within a narrow resonance bandwidth. The width of the spectrum is related to the detuning of the SPDC wavelength from the electric resonance; a strong enhancement is expected for metasurfaces with small detunings.

The generation of spatially entangled photon pairs through SPDC from a metasurface incorporating a nonlinear thin film of lithium niobate has been experimentally demonstrated in ref. [56]. The enhanced generation was achieved through nonlocal resonances with tailored angular dispersion mediated by an integrated silica meta-grating, enabling control of the emission pattern and associated quantum states of light by designing the grating profile and tuning the pump frequency (see Figure 3h). In such a metasurface, due to high-quality-factor of metasurface resonances, the photon-pair rate is strongly enhanced by 450 times as compared to unpatterned films (see Figure 3i). The correlations of photon positions were demonstrated through the violation of the classical Cauchy–Schwartz inequality (Figure 3j,k), witnessing the presence of multi-mode spatial entanglement.

The generation of tunable photon pairs via SPDC driven by high-Q quasi-BIC resonances in GaAs have been demonstrated in ref. [66]. A conceptual diagram of the process is presented in **Figure 4**a, while the structure of the metasurfaces is shown in Figure 4b: The addition of a small rectangle (pink) breaks the rotational symmetries C2, C4 of the metasurface, turning the BIC into a quasi-BIC resonance. Such kind of metasurfaces can emit frequency-degenerate and nondegenerate narrowband photon pairs tunable over more than 100 nm by changing either the optical pump or the spectral location of the resonances without appreciable loss of efficiency. In particular, it was demonstrated[66] that when the metasurface is illuminated by the pump whose doubled wavelength is non-resonant with respect to quasi-BIC modes, the SPDC spectrum exhibits two narrow peaks, one centered at the quasi-BIC wavelength (λ_{res} = 1359.4 nm) and the other at a partner wavelength (λ_1), in accordance with the energy conservation law (see Figure 4c). Such metasurfaces can be used to generate complex photon quantum states, including cluster states of light and multichannel single photons that could facilitate compact quantum information processing. Complex entanglement can be created using multiple pump beams. For example, in ref. [66], two pump beams at different wavelengths were used to produce pairs of entangled photons. The signal photons of both processes (λ_{res}) were emitted at the quasi-BIC resonance, while the idler photons were emitted at the correlated wavelengths (λ_1 and λ_2) which are out of the quasi-BIC resonance (see Figure 4c). By adding a third (multiple) pump which produces a photon pair at wavelengths λ_{res} and λ_3 (λ_n), more complicated graph states can be created, making metasurfaces promising universal sources for generating complex states of light that are an essential part of quantum information protocols.

4. Conclusions and Outlook

Recent advances in the rapidly developing field of dielectric nanoresonators and metasurfaces make such systems increas-

ingly attractive for various applications in quantum optics. The ability to obtain the desired optical properties by creating a proper geometric shape of subwavelength elements opens up an untapped potential for designing and manufacturing nanoresonators and metasurfaces to generate structured quantum light and provide an advanced control of its spectral and spatiotemporal properties. Rapid progress in the development of efficient nonlinear nanoresonators and metasurfaces has facilitated the advancements of nanoscale sources of quantum light generated via spontaneous parametric processes. Currently, the efficiency of biphoton generation in subwavelength systems is approaching practical levels opening up broad prospects for producing miniaturized sources of correlated quantum light. Such sources can further be integrated in large quantities into complex yet compact and energy efficient optical systems. The subwavelength architecture of metasurfaces provides many opportunities for generating quantum states characterized by strong entanglement. Further boost of the efficiency are envisioned by multiple approaches, including loss-based PT-symmetry which might find applications in nanoscale biphoton generation.[67]

The emerging field of implementing higher-order nonlinearities in nanostructured solids has a great potential for generating photon triplets and other high-order photon multiplets in metasurfaces and individual nanoresonators, which can be utilized as sources of multipartite entanglement.[68] With increasing generation efficiency, multiphoton squeezed light generation at the nanoscale might also become a reality.[69] Finally, nanostructured photonic sources can further be combined with other subwavelength systems to develop circuits for nanoscale quantum metrology as well as quantum information processing.

Acknowledgements

A.S.S. acknowledges support by the Australian Research Council (project No. DE180100070). S.S.K. acknowledges support from the EU Horizon 2020 research and innovation program (grant 896735) and the Australian Research Council (DE210100679). P.R.Sh. acknowledges support by the Deutsche Forschungsgemeinschaft (DFG) via TRR 142/3, Project C10, and via Project SH 1228/3-1.

Open access publishing facilitated by University of Technology Sydney, as part of the Wiley - University of Technology Sydney agreement via the Council of Australian University Librarians.

Conflict of Interest

The authors declare no conflict of interest.

Author Contributions

All authors contributed to literature review, analysis, and writing.

Keywords

dielectric nanoresonators, nanophotonics, spontaneous parametric down-conversion

Received: June 2, 2022
Revised: November 15, 2022
Published online: January 29, 2023

[1] J. L. O'Brien, A. Furusawa, J. Vučković, *Nat. Photonics* **2009**, *3*, 687.
[2] A. Aspuru-Guzik, P. Walther, *Nat. Phys.* **2012**, *8*, 285.
[3] I. A. Walmsley, *Science* **2015**, *348*, 525.
[4] J. Wang, S. Paesani, Y. Ding, R. Santagati, P. Skrzypczyk, A. Salavrakos, J. Tura, R. Augusiak, L. Mančinska, D. Bacco, D. Bonneau, J. W. Silverstone, Q. Gong, A. Acín, K. Rottwitt, L. K. Oxenløwe, J. L. O'Brien, A. Laing, M. G. Thompson, *Science* **2018**, *360*, 285.
[5] A. S. Solntsev, G. S. Agarwal, Y. Y. Kivshar, *Nat. Photonics* **2021**, *15*, 327.
[6] D. N. Klyshko, A. N. Penin, B. F. Polkovnikov, *Soviet Journal of Experimental and Theoretical Physics Letters* **1970**, *11*, 5.
[7] H. Takesue, K. Inoue, *Phys. Rev. A* **2004**, *70*, 031802.
[8] M. Massaro, E. Meyer-Scott, N. Montaut, H. Herrmann, C. Silberhorn, *New J. Phys.* **2019**, *21*, 053038.
[9] A. S. Solntsev, A. A. Sukhorukov, *Rev. Phys.* **2017**, *2*, 19.
[10] D. Leykam, A. S. Solntsev, A. A. Sukhorukov, A. S. Desyatnikov, *Phys. Rev. A* **2015**, *92*, 033815.
[11] A. S. Solntsev, G. K. Kitaeva, I. I. Naumova, A. N. Penin, *Appl. Phys. B* **2010**, *99*, 197.
[12] T. Liu, A. S. Solntsev, A. Boes, T. Nguyen, C. Will, A. Mitchell, D. N. Neshev, A. A. Sukhorukov, *Opt. Lett.* **2016**, *41*, 5278.
[13] F. Setzpfandt, A. S. Solntsev, J. Titchener, C. W. Wu, C. Xiong, R. Schiek, T. Pertsch, D. N. Neshev, A. A. Sukhorukov, *Laser Photonics Rev.* **2016**, *10*, 131.
[14] X. Guo, C.-l. Zou, C. Schuck, H. Jung, R. Cheng, H. X. Tang, *Light: Sci. Appl.* **2017**, *6*, e16249.
[15] G. Moody, L. Chang, T. J. Steiner, J. E. Bowers, *AVS Quantum Sci.* **2020**, *2*, 41702.
[16] A. S. Solntsev, F. Setzpfandt, A. S. Clark, C. W. Wu, M. J. Collins, C. Xiong, A. Schreiber, F. Katzschmann, F. Eilenberger, R. Schiek, W. Sohler, A. Mitchell, C. Silberhorn, B. J. Eggleton, T. Pertsch, A. A. Sukhorukov, D. N. Neshev, Y. S. Kivshar, *Phys. Rev. X* **2014**, *4*, 031007.
[17] X. Zambrana-puyalto, N. Bonod, *Phys. Rev. B* **2015**, *91*, 195422.
[18] S. Kruk, Y. Kivshar, *ACS Photonics* **2017**, *4*, 2638.
[19] P. A. Dmitriev, D. G. Baranov, V. A. Milichko, S. V. Makarov, I. S. Mukhin, A. K. Samusev, A. E. Krasnok, P. A. Belov, Y. S. Kivshar, *Nanoscale* **2016**, *8*, 9721.
[20] R. Camacho-Morales, M. Rahmani, S. Kruk, L. Wang, L. Xu, D. A. Smirnova, A. S. Solntsev, A. Miroshnichenko, H. H. Tan, F. Karouta, S. Naureen, K. Vora, L. Carletti, C. De Angelis, C. Jagadish, Y. S. Kivshar, D. N. Neshev, *Nano Lett.* **2016**, *16*, 7191.
[21] K. Frizyuk, M. Hasan, A. Krasnok, A. Alú, M. Petrov, *Phys. Rev. B* **2018**, *97*, 085414.
[22] R. Won, *Nat. Photonics* **2019**, *13*, 585.
[23] D. Rocco, A. Lamprianidis, A. E. Miroshnichenko, C. De Angelis, *J. Opt. Soc. Am. B* **2020**, *37*, 2738.
[24] V. Zubyuk, L. Carletti, M. Shcherbakov, S. Kruk, *APL Mater.* **2021**, *9*, 060701.
[25] M. Khorasaninejad, W. T. Chen, R. C. Devlin, J. Oh, A. Y. Zhu, F. Capasso, *Science* **2016**, *352*, 1190.
[26] Y. Yang, W. Wang, P. Moitra, I. I. Kravchenko, D. P. Briggs, J. Valentine, *Nano Lett.* **2014**, *14*, 1394.
[27] L. Wang, S. Kruk, H. Tang, T. Li, I. Kravchenko, D. N. Neshev, Y. S. Kivshar, *Optica* **2016**, *3*, 1504.
[28] K. Wang, J. G. Titchener, S. S. Kruk, L. Xu, H.-p. Chung, M. Parry, I. I. Kravchenko, Y.-h. Chen, A. S. Solntsev, Y. S. Kivshar, D. N. Neshev, A. A. Sukhorukov, *Science* **2018**, *361*, 1104.
[29] A. N. Poddubny, D. A. Smirnova, **2018**, arXiv:1808.04811.
[30] G. Marino, A. S. Solntsev, L. Xu, V. F. Gili, L. Carletti, A. N. Poddubny, M. Rahmani, D. A. Smirnova, H. Chen, A. Lemaître, G. Zhang, A. V. Zayats, C. D. Angelis, G. Leo, A. A. Sukhorukov, D. N. Neshev, *Optica* **2019**, *6*, 1416.
[31] T. J. Arruda, R. Bachelard, J. Weiner, S. Slama, P. W. Courteille, *Phys. Rev. A* **2020**, *101*, 023828.

[32] M. Parry, A. Mazzanti, A. Poddubny, G. D. Valle, D. N. Neshev, A. A. Sukhorukov, *New J. Phys.* **2022**, *24*, 035006.
[33] A. N. Poddubny, D. N. Neshev, A. A. Sukhorukov, in *Nonlinear Meta-optics*, CRC Press, Boca Raton, FL **2020**, Ch. 5. https://www.taylorfrancis.com/chapters/edit/10.1201/b22515-5/quantum-nonlinear-metasurfaces-alexander-poddubny-dragomir-neshev-andrey-sukhorukov?context=ubx&refId=34b8e111-287e-4f90-ba0a-57b2784fce85.
[34] K. Wang, M. Chekhova, Y. Kivshar, *Phys. Today* **2022**, *75*, 38.
[35] A. N. Poddubny, I. V. Iorsh, A. A. Sukhorukov, *Phys. Rev. Lett.* **2016**, *117*, 123901.
[36] M. R. Shcherbakov, D. N. Neshev, B. Hopkins, A. S. Shorokhov, I. Staude, E. V. Melik-Gaykazyan, M. Decker, A. A. Ezhov, A. E. Miroshnichenko, I. Brener, A. A. Fedyanin, Y. S. Kivshar, *Nano Lett.* **2014**, *14*, 6488.
[37] E. V. Melik-Gaykazyan, S. S. Kruk, R. Camacho-Morales, L. Xu, M. Rahmani, K. Zangeneh Kamali, A. Lamprianidis, A. E. Miroshnichenko, A. A. Fedyanin, D. N. Neshev, Y. S. Kivshar, *ACS Photonics* **2018**, *5*, 728.
[38] G. Grinblat, Y. Li, M. P. Nielsen, R. F. Oulton, S. A. Maier, *ACS Nano* **2017**, *11*, 953.
[39] K. Koshelev, S. Kruk, E. Melik-Gaykazyan, J.-H. Choi, A. Bogdanov, H.-G. Park, Y. Kivshar, *Science* **2020**, *367*, 288.
[40] A. P. Anthur, H. Zhang, R. Paniagua-Dominguez, D. A. Kalashnikov, S. T. Ha, T. W. W. Maß, A. I. Kuznetsov, L. Krivitsky, *Nano Lett.* **2020**, *20*, 8745.
[41] A. Zalogina, L. Carletti, A. Tripathi, H.-C. Lee, I. Shadrivov, H.-G. Park, K. Y. S. Kruk, in *CLEO2022*, Optica Publishing Group, Washington, DC **2022**, p. FF4N.8.
[42] H. Liu, C. Guo, G. Vampa, J. L. Zhang, T. Sarmiento, M. Xiao, P. H. Bucksbaum, J. Vučković, S. Fan, D. A. Reis, *Nat. Phys.* **2018**, *14*, 1006.
[43] C. Schlickriede, S. S. Kruk, L. Wang, B. Sain, Y. Kivshar, T. Zentgraf, *Nano Lett.* **2020**, *20*, 4370.
[44] S. Kruk, L. Wang, B. Sain, Z. Dong, J. Yang, T. Zentgraf, Y. Kivshar, *Nat. Photonics* **2022**, *16*, 561.
[45] S. Ghimire, D. A. Reis, *Nat. Phys.* **2019**, *15*, 10.
[46] M. F. Limonov, M. V. Rybin, A. N. Poddubny, Y. S. Kivshar, *Nat. Photonics* **2017**, *11*, 543.
[47] Y. Yang, I. I. Kravchenko, D. P. Briggs, J. Valentine, *Nat. Commun.* **2014**, *5*, 5753.
[48] K. Koshelev, A. Bogdanov, Y. Kivshar, *Sci. Bull.* **2019**, *64*, 836.
[49] G. Zograf, K. Koshelev, A. Zalogina, V. Korolev, R. Hollinger, D.-Y. Choi, M. Zuerch, C. Spielmann, B. Luther-Davies, D. Kartashov, S. V. Makarov, S. S. Kruk, Y. Kivshar, *ACS Photonics* **2022**, *9*, 567.
[50] M. R. Shcherbakov, H. Zhang, M. Tripepi, G. Sartorello, N. Talisa, A. AlShafey, Z. Fan, J. Twardowski, L. A. Krivitsky, A. I. Kuznetsov, E. Chowdhury, G. Shvets, *Nat. Commun.* **2021**, *12*, 4185.
[51] M. Müller, S. Bounouar, K. D. Jöns, M. Glässl, P. Michler, *Nat. Photonics* **2014**, *8*, 224.
[52] M. A. M. Versteegh, M. E. Reimer, K. D. Jöns, D. Dalacu, P. J. Poole, A. Gulinatti, A. Giudice, V. Zwiller, *Nat. Commun.* **2014**, *5*, 5298.
[53] C. Okoth, A. Cavanna, T. Santiago-Cruz, M. V. Chekhova, *Phys. Rev. Lett.* **2019**, *123*, 263602.
[54] A. Mazzanti, M. Parry, A. N. Poddubny, G. D. Valle, D. N. Neshev, A. A. Sukhorukov, *New J. Phys.* **2022**, *24*, 35006.
[55] T. Santiago-Cruz, A. Fedotova, V. Sultanov, M. A. Weissflog, D. Arslan, M. Younesi, T. Pertsch, I. Staude, F. Setzpfandt, M. Chekhova, *Nano Lett.* **2021**, *21*, 4423.
[56] J. Zhang, J. Ma, M. Parry, M. Cai, R. Camacho-Morales, L. Xu, D. N. Neshev, A. A. Sukhorukov, *Sci. Adv.* **2022**, *8*, eabq4240.
[57] N. A. Olekhno, M. I. Petrov, I. V. Iorsh, A. A. Sukhorukov, A. S. Solntsev, in *2022 Int. Conf. Laser Optics (ICLO)*, IEEE, Piscataway, NJ **2022**, p. 1.
[58] B. Jin, D. Mishra, C. Argyropoulos, *Nanoscale* **2021**, *13*, 19903.
[59] N. M. H. Duong, G. Saerens, F. Timpu, M. T. Buscaglia, V. Buscaglia, A. Morandi, J. S. Müller, A. Maeder, F. Kaufmann, A. S. Solntsev, R. Grange, *Opt. Mater. Express* **2022**, *12*, 3696.
[60] J. Zhao, C. Ma, M. Rüsing, S. Mookherjea, *Phys. Rev. Lett.* **2020**, *124*, 163603.
[61] A. S. Solntsev, A. A. Sukhorukov, D. N. Neshev, R. Iliew, R. Geiss, T. Pertsch, Y. S. Kivshar, *Appl. Phys. Lett.* **2011**, *98*, 231110.
[62] J.-C. Duan, J.-N. Zhang, Y.-J. Zhu, C.-W. Sun, Y.-C. Liu, P. Xu, Z. Xie, Y.-X. Gong, S.-N. Zhu, *J. Opt. Soc. Am. B* **2020**, *37*, 2139.
[63] D. Zhu, L. Shao, M. Yu, R. Cheng, B. Desiatov, C. J. Xin, Y. Hu, J. Holzgrafe, S. Ghosh, A. Shams-Ansari, E. Puma, N. Sinclair, C. Reimer, M. Zhang, M. Lončar, *Adv. Opt. Photon.* **2021**, *13*, 242.
[64] G.-T. Xue, Y.-F. Niu, X. Liu, J.-C. Duan, W. Chen, Y. Pan, K. Jia, X. Wang, H.-Y. Liu, Y. Zhang, P. Xu, G. Zhao, X. Cai, Y.-X. Gong, X. Hu, Z. Xie, S. Zhu, *Phys. Rev. Appl.* **2021**, *15*, 064059.
[65] L. Ebers, A. Ferreri, M. Hammer, M. Albert, C. Meier, J. Förstner, P. R. Sharapova, *J. Phys.: Photonics* **2022**, *4*, 025001.
[66] T. Santiago-Cruz, S. D. Gennaro, O. Mitrofanov, S. Addamane, J. Reno, I. Brener, M. V. Chekhova, *Science* **2022**, *377*, 991.
[67] D. A. Antonosyan, A. S. Solntsev, A. A. Sukhorukov, *Photon. Res.* **2018**, *6*, A6.
[68] H. Hübel, D. R. Hamel, A. Fedrizzi, S. Ramelow, K. J. Resch, T. Jennewein, *Nature* **2010**, *466*, 601.
[69] U. L. Andersen, T. Gehring, C. Marquardt, G. Leuchs, *Phys. Scr.* **2016**, *91*, 53001.

Polina R. Sharapova received her diploma in Physics in 2012 and Ph.D. degree in 2015 from M.V. Lomonosov Moscow State University. She is currently the Junior-Professor at Paderborn University and the head of the Theoretical Quantum Optics group. Her research interests include generation and manipulation of quantum states of light, multidimensional entanglement and macrocorrelations, integrated quantum technologies, matter–quantum light interaction, and semiconductor quantum optics.

Sergey Kruk is currently a senior lecturer and an Australian Research Council (ARC) DECRA Fellow at the Australian National University. His research interests are in nonlinear light–matter interactions in nanostructured solids. Dr. Kruk received his undergraduate degree (diploma) in Physics from the Belarusian State University in 2011 and his Ph.D. from the Australian National University in 2015, where he subsequently continued as a Research Fellow. Dr. Kruk has been a Humboldt Fellow (2019 award) and a Marie Skłodowska-Curie Fellow (2020 award) at the University of Paderborn, Germany.

Alex Solntsev has graduated with degrees in Physics and Education from Moscow State University and received a Ph.D. from Australian National University (ANU). He worked as a researcher at ANU until joining the University of Technology Sydney and starting a nonlinear optics lab as a DECRA Fellow. Now he leads research in nonlinear optics and works as an Associate Head of School Research for Mathematical and Physical Sciences.